Journal of Neuroscience Research 76:232–243 (2004)

Magnetic Resonance Tracking of Transplanted Bone Marrow and Embryonic Stem Cells Labeled by Iron Oxide Nanoparticles in Rat Brain and Spinal Cord

Pavla Jendelová,[1–3] Vít Herynek,[4] Lucia Urdzíková,[2] Kateřina Glogarová,[1,2] Jana Kroupová,[2,5] Benita Andersson,[2,6] Vítězslav Bryja,[1,2] Martin Burian,[4] Milan Hájek,[4] and Eva Syková[1–3]*

[1]Institute of Experimental Medicine Academy of Sciences of the Czech Republic, Prague, Czech Republic
[2]Center for Cell Therapy and Tissue Repair, Charles University, Second Medical Faculty, Prague, Czech Republic
[3]Department of Neuroscience, Charles University, Second Medical Faculty, Prague, Czech Republic
[4]MR-Unit, Radiology Department, Institute for Clinical and Experimental Medicine, Prague, Czech Republic
[5]Mendel University, Brno, Czech Republic
[6]Department of Clinical Neuroscience, Karolinska Institutet, Stockholm, Sweden

Nuclear magnetic resonance (MR) imaging provides a noninvasive method for studying the fate of transplanted cells in vivo. We studied, in animals with a cortical photochemical lesion or with a balloon-induced spinal cord compression lesion, the fate of implanted rat bone marrow stromal cells (MSCs) and mouse embryonic stem cells (ESCs) labeled with superparamagnetic iron oxide nanoparticles (Endorem). MSCs were colabeled with bromodeoxyuridine (BrdU), and ESCs were transfected with pEGFP-C1 (eGFP ESCs). Cells were either grafted intracerebrally into the contralateral hemisphere of the adult rat brain or injected intravenously. In vivo MR imaging was used to track their fate; Prussian blue staining and electron microscopy confirmed the presence of iron oxide nanoparticles inside the cells. During the first week postimplantation, grafted cells migrated to the lesion site and populated the border zone of the lesion. Less than 3% of MSCs differentiated into neurons and none into astrocytes; 5% of eGFP ESCs differentiated into neurons, whereas 70% of eGFP ESCs became astrocytes. The implanted cells were visible on MR images as a hypointense area at the injection site, in the corpus callosum and in the lesion. The hypointense signal persisted for more than 50 days. The presence of GFP-positive or BrdU-positive and nanoparticle-labeled cells was confirmed by histological staining. Our study demonstrates that both grafted MSCs and eGFP ESCs labeled with a contrast agent based on iron oxide nanoparticles migrate into the injured CNS. Iron oxide nanoparticles can therefore be used as a marker for the long-term noninvasive MR tracking of implanted stem cells.

Key words: cell transplantation; magnetic resonance; contrast agents; injury; photochemical lesion; spinal cord lesion

New possibilities for repairing nervous system damage have opened after the discovery that stem cells can differentiate into neural tissue in the adult brain (Gage, 2002; Taupin and Gage, 2002; van Praag et al., 2002). Considerable progress has been made in developing effective methods for culturing different types of stem cells and transplanting them into animal models of degenerative disorders, ischemia, or injury (Bjorklund et al., 2003; Isacson, 2003; Silani and Leigh, 2003). The transplanted cells could directly replace lost populations of cells, such as neurons or glia, or they could provide factors that facilitate the regeneration of host cells.

Investigations of the success of cell-based therapies have so far required the analysis of brain sections postmortem. This method, therefore, does not yield data on the fate and time course of the migration of the transplanted stem cells in the host organism. Labeling of the cultured cells with superparamagnetic iron oxide nanopar-

Contract grant sponsor: Ministry of Education, Sports and Youth of the Czech Republic; Contract grant numbers: LN00A065 and J13/98: 11120004.

Contract grant sponsor: Academy of Sciences of the Czech Republic; Contract grant number: AVOZ5039906-1024.

Contract grant sponser: Grant Agency of the Czech Republic; Contract grant number: 304/03/1189.

*Correspondence to: Prof. Eva Syková MD, DSc, Institute of Experimental Medicine ASCR, Videňská 1083, 140 20 Prague 4, Czech Republic. E-mail: sykova@biomed.cas.cz

Received 3 October 2003; Revised 23 October 2003; Accepted 5 November 2003

Published online 8 March 2004 in Wiley InterScience (www.interscience.wiley.com). DOI: 10.1002/jnr.20041

ticles and the use of magnetic resonance imaging (MRI) provide a noninvasive method for studying the fate of transplanted cells in vivo (Bulte et al., 1999a, 2001; Jendelová et al., 2003). The cells can be labeled by nanoparticle contrast agents during their incubation in cell culture before transplantation into the tissue.

Superparamagnetic contrast agents are formed by a superparamagnetic core, which is represented by iron oxide crystalline structures described by the general formula Fe_2O_3 $M^{2+}O$, where M is a divalent metal ion (M = Fe^{2+}, Mn^{2+}). For the synthesis of the contrast agents, small crystals of magnetite Fe_2O_3FeO are predominantly used. During the preparation of the contrast agent, the crystals are covered by a macromolecular shell, formed by dextran, starch and polyol derivatives, and other polymers, which can be chemically or biochemically modified (Yeh et al., 1993, 1995; Weissleder et al., 1997; Wang et al., 2001). When specific antibodies are attached to the shell, the contrast agent can be specifically bound to tissue (for review see Bulte and Bryant, 2001).

The use of a nanoparticle contrast agent in MRI leads to the shortening of both T1 and T2 relaxation times by an order of magnitude greater than that seen with standard paramagnetic contrast agents. Thus, it is possible to observe contrast changes on a cellular level by MR mini-imaging and MR microscopy techniques. Here we describe the in vivo MR tracking of implanted mouse embryonic stem cells (ESCs) and rat bone marrow stromal cells (MSCs) in rats with a cortical photochemical lesion (Jendelová et al., 2003) or a balloon-induced spinal cord compression lesion.

MATERIALS AND METHODS

Cell Culture and Iron Labeling

ESCs. D3 ESCs, a commercially available ES cell line (Doetschman et al., 1985), were transfected by using the electroporation method with 10 μg of pEGFP-C1 vector. Transfected cells were selected in medium containing 300 μg/ml of G418, cloned and termed *eGFP ESCs*. Fibroblasts of the feeder layer were removed by gradual rarefaction. Cells were grown in a humidified atmosphere with 5% CO_2 at 37°C in Dulbecco's modified Eagle medium (DMEM; Gibco, Paisley, Scotland) supplemented with 20% fetal calf serum (PAA Laboratories GmbH, Linz, Austria), 0.1 mM 2-mercaptoethanol (Sigma, St. Louis, MO), 1% nonessential amino acid stock (Gibco), 100 U/ml penicillin, 100 U/ml streptomycin (Gibco), and 1,000 U/ml recombinant mouse leukemia inhibitory factor (LIF; Chemicon International, Temecula, CA).

Neural differentiation was induced by culturing eGFP ESCs in serum containing DMEM/F12 without LIF for 2 days and then transferring the cells into serum-free media supplemented with insulin, transferrin, selenium, and fibronectin (ITSF) for further culture (Pachernik et al., 2002). After 12 days in ITSF media, the cells expressed N-CAM, GAP-43, GFAP, and MAP2. Cells were transplanted on the eighth day of differentiation, when differentiation had been initiated but these markers were not yet expressed.

Feeder-free eGFP ESCs were labeled with 112.4 mg/ml superparamagnetic iron oxide nanoparticles (Endorem, Guerbet, France) in three passages. Transplanted cells were detected by staining for iron to produce ferric ferrocyanide (Prussian blue) and by GFP fluorescence.

MSCs. For the isolation of rat MSCs, we used the method described by Jendelová et al. (2003). Briefly, femurs were dissected from 4-week-old Wistar rats. Marrow cells were plated in 80-cm^2 tissue culture flasks in DMEM/10% fetal bovine serum (FBS), with 100 U/ml penicillin and 100 U/ml streptomycin. After six to ten passages, the cells were implanted as a cell suspension. In culture, the cells were positive for CD90 and fibronectin and negative for CD11b and CD45.

An Endorem suspension (200 μl/20 ml of culture medium, i.e., 2.2 mg of iron) was added to the culture of rat MSCs 5 days prior to transplantation. After 72 hr, the contrast agent was washed out. The rat MSCs were colabeled with 5 μM BrdU (Sigma) 24 hr prior to transplantation.

Experimental Animals

Wistar rats, 6–8 weeks old, were used throughout the study. Animals were divided into the following groups: 1) rats with a cortical photochemical lesion and with contralaterally grafted nanoparticle-labeled eGFP ESCs (n = 12); 2) rats with a cortical photochemical lesion and with contralaterally grafted nanoparticle and BrdU colabeled rat MSCs (n = 15); 3) rats with a cortical lesion and with nanoparticle-labeled eGFP ESCs administered intravenously (n = 7); 4) rats with a cortical lesion and with nanoparticle- and BrdU-colabeled rat MSCs administered intravenously (n = 12); 5) rats with a cortical photochemical lesion and with contralaterally injected contrast agent Endorem (n = 3); 6) rats with a balloon-induced spinal cord compression lesion and with nanoparticle-labeled rat MSCs administered intravenously (n = 8); and 7) rats with cortical lesion or balloon-induced compression lesion injected with phosphate-buffered saline (PBS) into the contralateral hemisphere or intravenously (n = 12).

Photochemical Lesion

We used a photochemical lesion as a model of thrombotic stroke (Watson et al., 1985). The model uses a photochemical reaction in vivo to induce a thrombosis leading to a cerebral infarction. The method is virtually noninvasive, because the skull is translucent for light at 560 nm, which is the wavelength used for inducing the photochemical reaction. The rats were anesthetized with isoflorane (2% isoflorane in air). Rose Bengal, a potent photosensitizing dye, was injected intravenously into the femoral vein (1 mg/100 g). A 1- × 2-mm area of the skull above the right cortex was exposed to the light from a halogen lamp for 10 min, while the rest of the skull was shielded with aluminium foil. Rose Bengal is excited and subsequently generates singlet molecular oxygen, so it has the ability to induce photoperoxidative reactions. Damage to lipid membranes may provide the initial stimulus for platelet adhesion and subsequent aggregation, leading to thrombosis and infarction within 1 hour (Watson et al., 1985). The formation of thrombotic plugs and adjacent red blood cell stasis within pial and parenchymal vessels is thus observed within the irradiated zone. The rats were left to recover and returned to their cages.

Balloon-Induced Spinal Cord Compression Lesion

Balloon-induced spinal cord compression lesion is a simple and reproducible lesion. The method was described in detail by Vanicky et al. (2001). Briefly, a 2-French Fogarty catheter was inserted into the dorsal epidural space through a small hole made in the Th10 vertebral arch. A spinal cord lesion was made by balloon inflation (volume 15 μl) at the Th8–Th9 spinal level. Inflation for 5 min produced paraplegia, and this was followed by gradual recovery.

Grafting of eGFP ESCs and MSCs

Rats were anesthetized with isoflorane 7 days after the photochemical lesion and mounted in a stereotactic frame. With aseptic techniques, a burr hole (1 mm) was made on the left side of the skull to expose the dura overlying the left cortex (Jendelová et al., 2003). To reduce the risk of tumor formation, eGFP ESCs induced into neural differentiation or MSCs (2×10^5) were suspended in 5 μl of PBS and slowly injected over a 10-min period using a Hamilton syringe into the contralateral hemisphere at AP = –1 mm, ML = 2.5 mm, and DV = 3.5 mm from bregma based on the atlas of Paxinos and Watson (1986). The opening was closed by bone wax and the skin sutured. For intravenous injection, approximately 2×10^6 undifferentiated eGFP ESCs or MSCs in 0.5 ml PBS were injected into the femoral vein. The vein was compressed for a short time to reduce bleeding and the wound sutured. An immunosuppressive agent (Depo-Medrol; Upjohn) was administered weekly.

MRI

MR images of the brain were obtained by using a 4.7-T Bruker spectrometer equipped with a homemade surface coil. The rats were anesthetized by passive inhalation of 1.5–2% isoflorane in air. Breathing was monitored during the measurements. Single sagittal, coronal, and transversal images were obtained by a fast-gradient echo sequence for localizing the subsequent T_2-weighted transversal images measured by a standard turbospin echo sequence. Sequence parameters were: repetition time (TR) = 2000 msec, effective echo time (TE) = 42.5 msec, turbo factor = 4, number of acquisitions (AC) = 16, field of view (FOV) = 3.5 cm, matrix 256 × 256, slice thickness 0.5 mm, slice separation 1 mm. Two sets of interleaved transversal images were measured to cover the whole brain (Jendelová et al., 2003).

MR images of the spinal cord were obtained by using a 4.7-T Bruker spectrometer equipped with standard whole-body resonator. The segments of spine fixed ex vivo with paraformaldehyde were placed in a 50-ml polypropylene test tube and then centered within the magnet. A 3D gradient echo sequence was used for data acquisition. Sequence parameters were: TR = 25 msec, TE = 5.1 msec, and AC = 128. The 3D slab was oriented sagittaly with the dimensions: FOV = 6 × 3 × 2.4 cm, matrix 256 × 128 × 96. Oblique projections (with respect to the magnet axes) were then reconstructed within the Paravision acquisition and processing software package (Bruker, Germany) to obtain the anatomically relevant planes. Phantoms containing labeled cells were measured by a similar sequence with different geometry: FOV = 6 cm, matrix 256 × 256, slice thickness 1 mm. Only one slice was measured in the case of phantoms.

Histology and Immunohistochemistry

In culture, the cells were immunohistochemically stained for CD90, fibronectin (Chemicon), and CD45 and CD11b (Pharmingen, San Diego, CA) by using monoclonal antibodies. As a secondary antibody, goat anti-mouse IgG Alexa 594 (Molecular Probes, Eugene, OR) was used. Rats were sacrificed 2–7 weeks after transplantation. The anesthetized animals were perfused with 4% paraformaldehyde in 0.1 M PBS (pH 7.4). Fixed brains were dissected and immersed in PBS with 30% sucrose. Frozen coronal sections (40 μm) were cut through the areas of interest.

Transplanted eGFP ESCs were detected by staining for iron to produce ferric ferrocyanide (Prussian blue) and by GFP fluorescence. To visualize the possible colocalization of GFP and cell-type-specific markers in the same cells, double staining was employed. Sections were incubated with cell-type-specific antibodies directed against a neuronal nuclear antigen (NeuN), dilution 1:100 (Chemicon), or against glial fibrilary acidic protein (GFAP) for identifying astrocytes, dilution 1:2,500 (Dako, Glostrup, Denmark). A fluorescein-conjugated secondary antibody (goat anti-mouse IgG Alexa 594) was used as the second label in the double-staining experiments.

Transplanted MSCs were detected by staining for iron to produce ferric ferrocyanide (Prussian blue) and by anti-BrdU staining using a monoclonal antibody (Roche, Mannheim, Germany). As a secondary antibody, goat anti-mouse IgG Alexa 594 (Molecular Probes) was used.

Electron Microscopy

For electron microscopic examination, undifferentiated eGFP ESCs or tissue with a cortical photochemical lesion was fixed at 4°C in 2.5% buffered glutaraldehyde for 1 hr, followed by 1% osmium tetroxide for 2 hr. The cells were dehydrated in ascending concentrations of ethanol, immersed in propylene oxide, and embedded in the resin Epon 812 (Agar Scientific Ltd., Standsted, England). The samples were cut into ultrathin sections (~60 nm), and these sections were contrasted with 4% uranyl acetate and Reynold's lead citrate and examined in a Philips Morgagni 268 transmission electron microscope.

Iron Content Quantitative Analysis

The amount of iron present in the cells was determined after mineralization by spectrophotometry. Two-milliliter samples containing 60 million cells were mineralized after the addition of 5 ml HNO_3 and 1 ml H_2O_2 in an ETHOS 900 microwave mineralizator (Millestone ETHOS 900, Sydney, Australia). Deionized water was added to reach a total volume of 100 ml. The iron content was determined with a Spectroflame M120S (Spectro Inc., Littleton, MA) calibrated in a standard solution of Astasol (Analytika Ltd., Prague, Czech Republic). The measurements were repeated four times, and the average mean value was determined. All experiments were carried out in accordance with the European Communities Council Directive of 24 November 1986 (86/609/EEC).

RESULTS

Implantation of ESCs

Labeling of eGFP ESCs with iron oxide nanoparticles. eGFP ESCs were incubated with iron oxide nanoparticles (Endorem) for three passages. Iron inside the

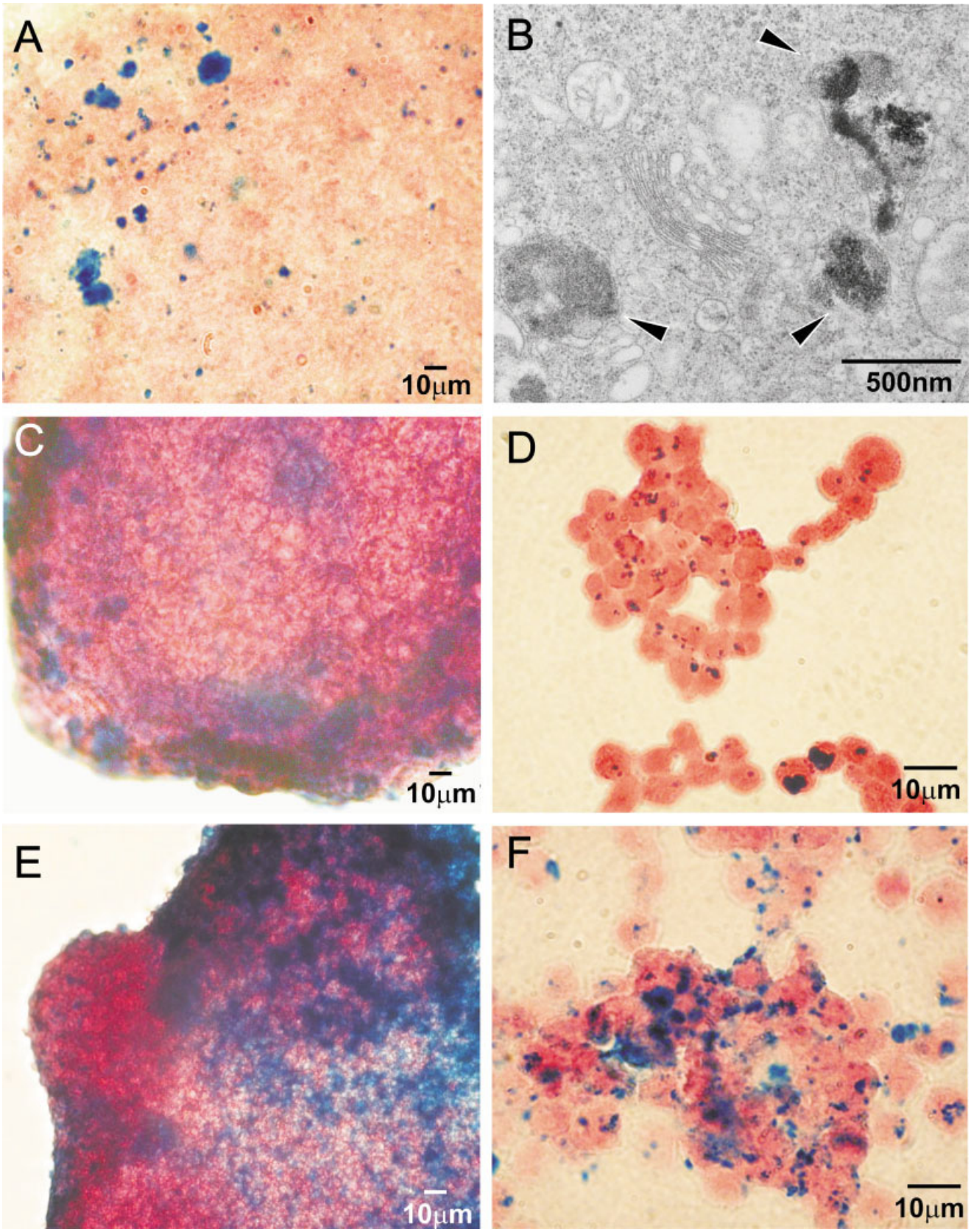

Fig. 1. eGFP ESC labeling with iron oxide nanoparticles. **A,C,E:** A colony of eGFP ESCs in culture labeled with iron oxide nanoparticles (Prussian blue staining); first, second, and third passages, respectively. **B:** Transmission electron microphotograph showing a cluster of iron nanoparticles surrounded by a cell membrane in the close vicinity of the Golgi apparatus (arrowheads), confirming the presence of iron inside the cell. **D,F:** Trypsinized nanoparticle-labeled cell suspensions of ESCs after the second and third passages, respectively. Note that, after the third passage, the intensity of Prussian blue staining increased, indicating a greater number of iron nanoparticles inside the cells.

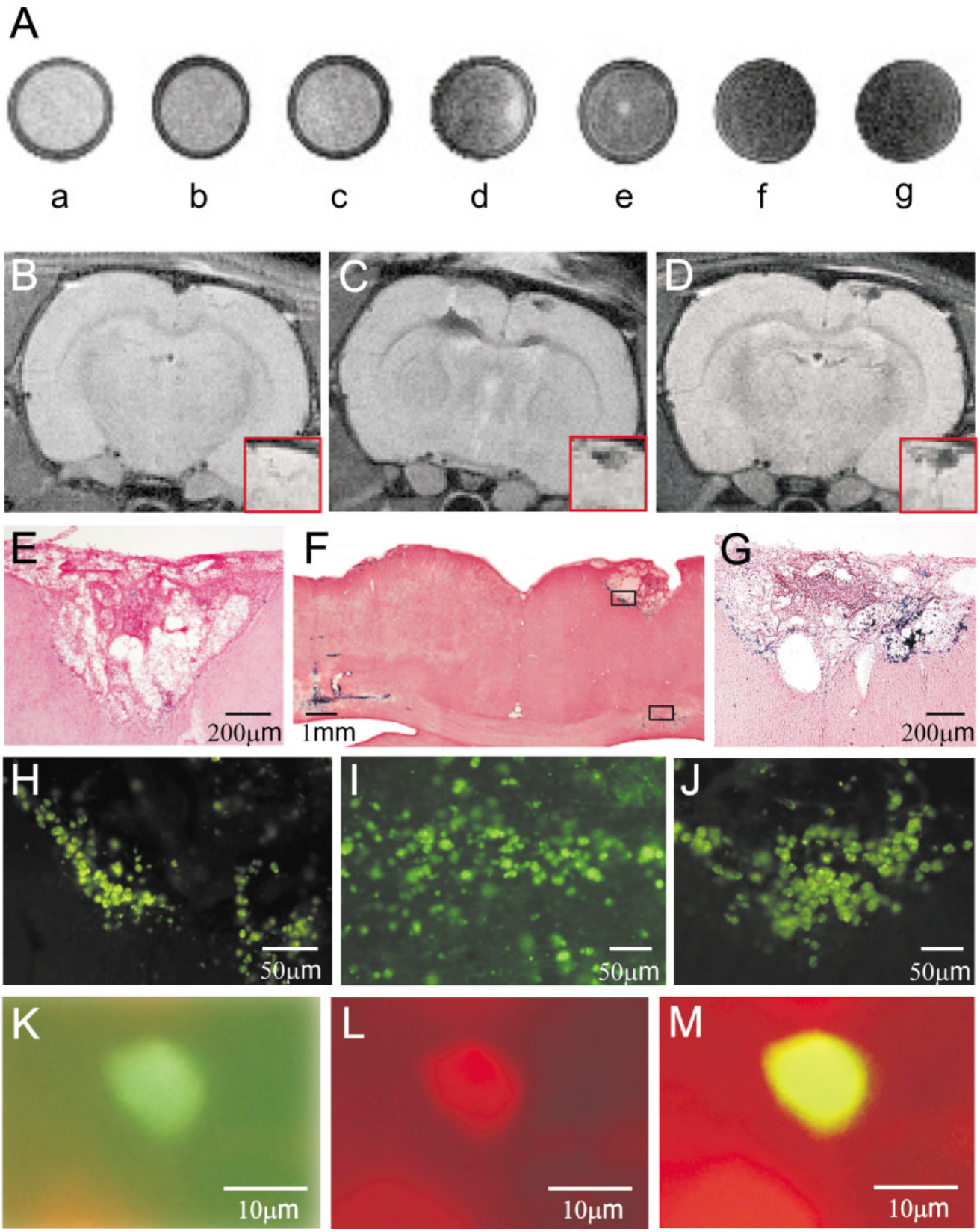
A
a
b
c
d
e
f
g
B
C
D
E
200μm
F
1mm
G
200μm
H
50μm
I
50μm
J
50μm
K
10μm
L
10μm
M
10μm

Figure 2.

cells was visualized by Prussian blue staining. The iron oxide nanoparticles in colonies of eGFP ESCs in culture were observed as blue spots with an optical microscope (Axioskop, Zeiss; Fig. 1). Cell counting of Prussian blue-stained cells in cell suspension revealed that, after the first passage, 40.9% ± 5.9% of cells were labeled (Fig. 1A), after the second passage 84.3% ± 7.0% (Fig. 1C,D), and after the third passage 81.0% ± 6.1% (Fig. 1E,F). The third passage did not increase the number of labeled cells; however, the number of iron particles inside the cells increased (Fig. 1F). Further passages did not increase either the number of labeled cells or the number of iron particles inside the cells. A colorimetric assay for the quantification of cell proliferation and cell viability based on the cleavage of the tetrazolium salt WST-1 (Roche Molecular Biochemicals) by mitochondrial dehydrogenases in viable cells did not show any differences between nanoparticle-labeled and nonlabeled cell groups.

Transmission electron microscopy confirmed the presence of iron oxide nanoparticles inside the cells, observed as membrane-bound clusters within the cell cytoplasm (Fig. 1B). Vesicles containing nanoparticles surrounded by a membrane indicated an endocytotic process of iron uptake. The mean iron concentration in a 2-ml sample containing 60 million cells was 8.2 μg/ml, which corresponds to an average value of 13.6 pg iron per cell.

In vitro MRI detection of ESCs. To check the sensitivity of the MRI technique and to mimic the signal behavior in brain tissue, we performed in vitro imaging of labeled cells. ESCs were labeled with Endorem as described above, and a cell suspension (at concentrations of 10,000, 5,000, 2,500, 1,250, 625, and 315 cells/μl) was suspended in 1.7% gelatin. MR images showed a clear hypointense signal at all concentrations greater than 315 cells per μl (Fig. 2A), which means that contrast changes were visible when approximately 17 or more cells were in the nominal pixel (0.055 μl).

Fate of grafted cells. We implanted eGFP ESCs into the cortex or injected them intravenously into the femoral vein. For rats with a cortical photochemical lesion, we found a massive migration of nanoparticle-labeled GFP-positive cells into the lesion site regardless of the route of administration.

In control animals without any implanted cells, the lesion was visible on MR images 2 hr after light exposure as a light-hyperintensive area, which remained visible during the whole measurement period, i.e., for 5 weeks (Fig. 2B). Only a few cells weakly stained for Prussian blue were found in photochemical lesions without any implanted cells (Fig. 2E). The staining represents iron, which most likely originated in hemorrhages and iron degradation products released from iron-containing proteins (such as hemoglobin, ferritin, and hemosiderin) and phagocytized by microglia/macrophages. We did not observe any GFP-positive cells in brains of nongrafted animals.

On MR images of brains with a photochemical lesion and contralaterally injected cells, the cell implants were clearly visible as a hypointense area at the injection site (Fig. 2C). Two weeks after grafting, a hypointense signal was also observed in the corpus callosum. At the same time, histology showed that a large number of Prussian blue-positive and GFP-labeled cells had entered the lesion (Fig. 2F,H). Many labeled cells were also detected in the corpus callosum, suggesting a migration from the contralateral hemisphere toward the lesion (Fig. 2F,I). In 10% of experiments, we observed hyperproliferation suggesting the formation of a tumor-like structure at the injection site, originating from GFP-positive cells. These tumors were visible on MR images as a large, hypointense area at the injection site, much larger than the regular cell implants.

After intravenous injection of eGFP ESCs, we found a hypointense MRI signal only at the site of the lesion (Fig. 2D). The first changes in the hypointensity of the MRI signal in the lesion were observed 1 week after cell injection. The hypointense signal in the lesion reached its maximum at about 2 weeks and persisted with no apparent decrease in signal intensity for the next 2 weeks. Histology confirmed the presence of Prussian blue-stained and GFP-positive cells in the lesion (Fig. 2G,J).

Electron microscopy showed iron oxide nanoparticles in brain tissue samples from lesioned rats transplanted with eGFP ESCs (Fig. 3). In tissue from brains with labeled eGFP ESCs implanted contralaterally to the lesion, the nanoparticles were observed in dense clusters in the cell cytoplasm. Figure 3A,B shows a typical astrocyte from lesioned tissue with the nanoparticles in small dense clusters in the cell cytoplasm, whereas Figure 3C,D shows an oligodendrocyte from the lesioned area with nanoparticles incorporated in membrane-bound clusters. In rats injected intravenously with labeled eGFP ESCs, the nanoparticles

Fig. 2. T2-weighted images of phantoms, cortical photochemical lesion, and implanted eGFP ESCs labeled with nanoparticles. **A:** MR images of phantoms showing a set of test tubes containing a suspension of nanoparticle-labeled eGFP ESCs in gelatin (sample a contains no cells; b, 315; c, 625; d, 1,250; e, 2,500; f, 5,000; g, 10,000 cells/μl). Nonhomogeneities in the phantom images are caused by the moderate sedimentation of cells while the gelatin was setting. **B:** A cortical photochemical lesion is visible on MR images 2 weeks after induction as a hyperintense area with sharp hypointense borders. **Inset** shows a higher magnification view of the lesion. **C:** Cell implant (in the hemisphere contralateral to the lesion) and the lesion are hypointense in MR images 2 weeks after implantation. A hypointensive signal is also found in the corpus callosum. **Inset** shows a higher magnification view of the lesion. **D:** A hypointense signal in the lesion 2 weeks after the intravenous injection of nanoparticle-labeled eGFP ESCs. **Inset** shows a higher magnification view of the lesion. **E:** A few cells weakly stained for Prussian blue are found in the photochemical lesion in animals without implanted cells. **F:** Dense Prussian blue staining of an injection site in the contralateral hemisphere, the corpus callosum, and a photochemical lesion, 4 weeks after grafting. **G:** Massive invasion of Prussian blue-stained cells into the lesion 4 weeks after the intravenous injection of eGFP ESCs. **H,I:** Higher magnification microphotograph of GFP-labeled cells showing GFP-positive ESCs in the lesion and in the corpus callosum (serial section to the slice shown in Fig. 2F). **J:** Higher magnification of GFP-positive cells in the lesion after intravenous injection of eGFP ESCs labeled with nanoparticles (serial section to the slice shown in Fig. 2G). **K,L:** Implanted eGFP ESCs at the border of the lesion 4 weeks after grafting, doubly stained for GFP (green) and the neuronal marker NeuN (red). **M:** Coexpression of both markers appears as yellow.

were found mostly in cells at the lesion border. The nanoparticles were either incorporated in lysosomes or distributed in large membrane-bounds clusters. In some cells (Fig. 3E,F, showing a neuron), nanoparticles were also apposed to the nuclear membrane.

Electron microscopy revealed that, of all the eGFP ESCs containing nanoparticles found in the lesion, 70% were astrocytes, very few (less than 1%) were oligodendrocytes (Fig. 3A–D), and 5% of nanoparticle-labeled eGFP ESCs had differentiated into neurons (Fig. 3E,F). Double staining for NeuN confirmed the expression of a neuronal marker in this population of eGFP ESCs (Fig. 2K–M). The rest of the cells remained undifferentiated.

To exclude the possibility that nanoparticles were taken up by endogenous cells, we injected the contrast agent alone, contralaterally to the lesion. We did not observe any neurons, astrocytes, or oligodendrocytes in the lesioned area that had incorporated nanoparticles into their cell cytoplasm.

Implantation of MSCs

Iron oxide-labeled MSCs in culture. Prussian blue-positive staining was found in virtually all MSCs incubated for 48–72 hr with Endorem (Fig. 4A). The average value of iron was 17.5 pg/cell (Jendelová et al., 2003). Transmission electron microscopy confirmed the presence of 20–30 iron oxide particles inside the cell, observed as endoplasmatic reticulum membrane-bound clusters within the cell cytoplasm (Fig. 4B).

Grafting of nanoparticle-labeled MSCs into rats with a cortical lesion. Nanoparticle/BrdU-colabeled MSCs were grafted into rats with a cortical photochemical lesion. One week after implantation, the cells massively populated the border zone of the damaged cortical tissue and were localized in the injured tissue around the necrotic part of the photochemical lesion. Only few (less than 3%) of the cells that migrated into the lesion expressed the neuronal marker NeuN when tested four weeks postimplantation (Fig. 4I–K). No GFAP-positive cells were found in the lesion (Jendelová et al., 2003).

Rats with grafted nanoparticle/BrdU-colabeled cells were examined weekly for a period of 3–7 weeks posttransplantation with an MR imager. No recognizable hypointense signal in the lesion was detected during the first 2 days after implantation. A decrease in the MR signal was found only at the injection site in animals with cells injected contralateraly to the lesion. One week after grafting, we observed a hypointense signal in the lesion, which intensified during the second and third weeks (Fig. 4C). Histology confirmed that a large number of Prussian blue-positive cells had entered the lesion (Fig. 4D,E). No hypointense signal was found in other brain regions. The hypointense signal occured only in damaged areas populated with MSCs, and its intensity corresponded to Prussian blue or BrdU staining (Jendelová et al., 2003).

After intravenous injection of MSCs, we obtained similar MR images. A decrease in the signal was observed 6 days after cell infusion and persisted for 7 weeks (Fig. 4F). Prussian blue and anti-BrdU staining confirmed the presence of iron oxide/BrdU-colabeled cells in the lesion (Fig. 4G,H; Jendelová et al., 2003).

Grafting of nanoparticle-labeled MSCs into rats with a spinal cord lesion. We used as a model of spinal cord injury a balloon-induced compression lesion. MSCs labeled with nanoparticles were injected intravenously into the femoral vein 1 week after lesioning ($n = 8$). MR images were taken ex vivo 4 weeks after cell implantation by using a 4.7-T Bruker spectrometer equipped with a standard whole-body resonator.

With MR images, we observed the lesion as a sharply bounded area with a hypointense signal in the area of the spinal channel (Fig. 5A,C). Images of transversal as well as longitudinal spinal cord sections from all grafted animals showed the lesion as a dark hypointense area (Fig. 5B,D). Prussian blue staining confirmed a large number of Prussian blue-positive cells present in the lesion (Fig. 5E,F). Compared with the case in control rats, in grafted animals the lesion, which was populated by grafted MSCs, was considerably smaller, suggesting the possibility of a positive effect of the MSCs on lesion repair (Fig. 5G,H). Our preliminary data with behavioral testing (BBB score and plantar test) indicate that lesioned animals with grafted MSCs have higher scores on BBB testing and show better responses in the plantar test than do control animals. However, further testing of more animals in the respective groups will be required to confirm these preliminary observations.

DISCUSSION

Our study shows that MRI techniques can be used to monitor the fate of transplanted stem cells in the host organism. Both mouse ESCs and rat MSCs can be labeled in vitro by superparamagnetic nanoparticles (Endorem) without lipofection and remain viable in culture or when implanted into the brain or spinal cord of rats. The distribution of the labeled cells can be monitored by MRI at regular intervals after implantation. The MRI technique can thus provide information about the migration and fate of the transplanted cells in nervous tissue. The data obtained from MRI correlated well with histological and electron microscopy findings. Our results are in agreement with the findings of Hoehn et al. (2002), who reported that magnetically labeled undifferentiated mouse ESCs injected intracerebrally can migrate into an ischemic lesion induced by middle cerebral artery occlusion. Cells, which were labeled with the contrast agent Sinerem (Guerbet, France), required lipofection, however. Several other groups have reported that it is possible to visualize magnetically labeled cells in the brain after transplantation. This includes rat fetal brain cells labeled with superparamagnetic iron oxide (SPIO) linked to lecitin wheat germ agglutinin (Norman et al., 1992), rat fetal brain tissue labeled with SPIO-containing reconstituted Sendai virus envelopes (Hawrylak et al., 1993), and CG-4 oligodendrocyte progenitor cells labeled with plain dextran-coated SPIO (Franklin et al., 1999). In these studies, the MRI contrast remained primarily localized at the injection site, and no widespread migration of cells was observed. Bulte et al. (1999b) reported the migration of CG-4 oligodendrocyte progenitor cells labeled with MION-461-OX-26

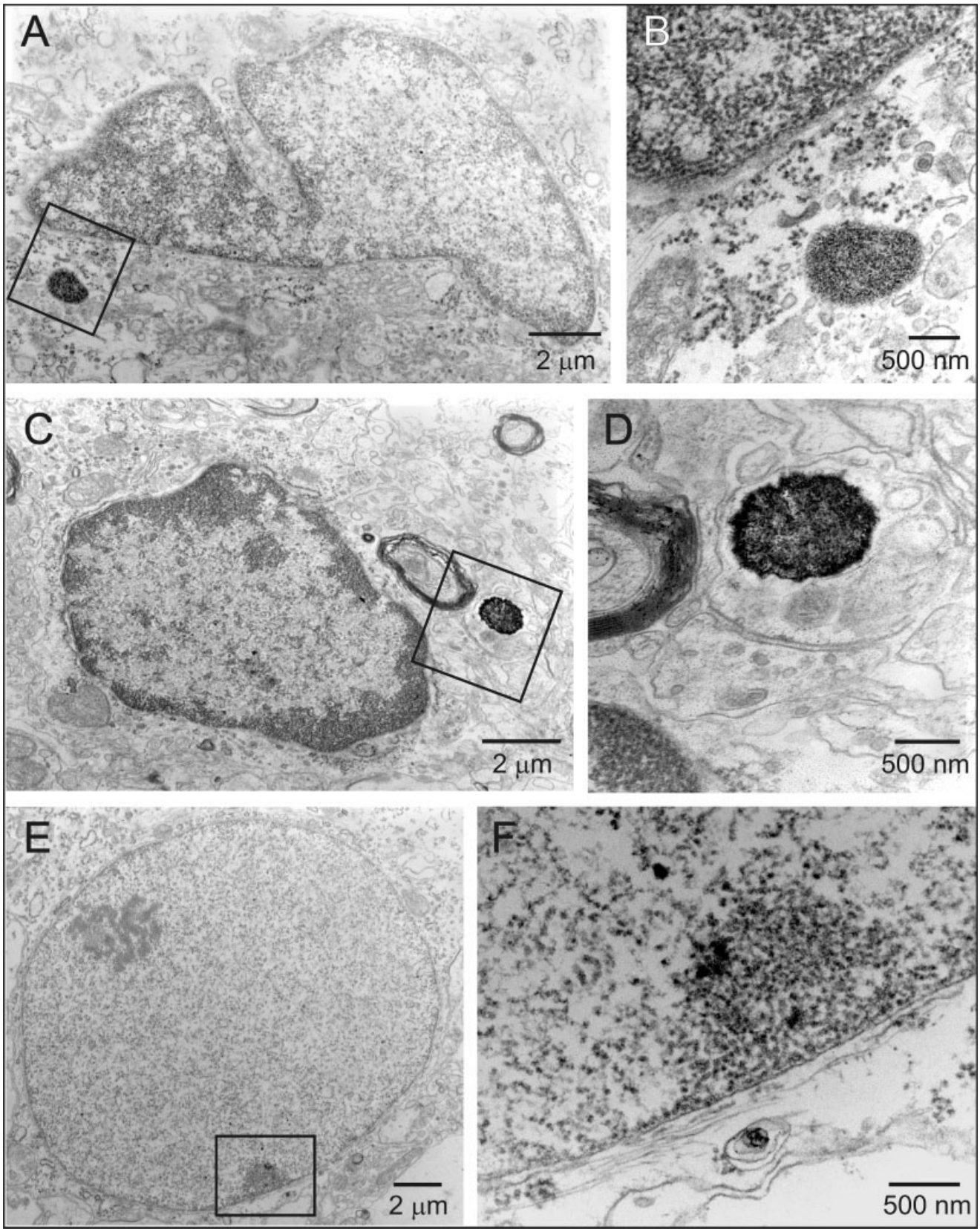

Fig. 3. Electron microphotographs of eGFP ESCs 4 weeks after implantation. **A,B:** Astrocyte from the brain tissue of a rat with nanoparticle-labeled eGFP ESCs implanted contralaterally to the lesion; the nanoparticles were observed in small, dense clusters in the cell cytoplasm. Boxed area in A is shown at higher magnification in B. **C,D:** Oligodendrocyte from the lesioned area having nanoparticles incorporated in membrane-bound clusters. Boxed area in C is shown at higher magnification in D. **E,F:** Neuron with nanoparticles marginated to the nuclear membrane. Boxed area in E is shown at higher magnification in F.

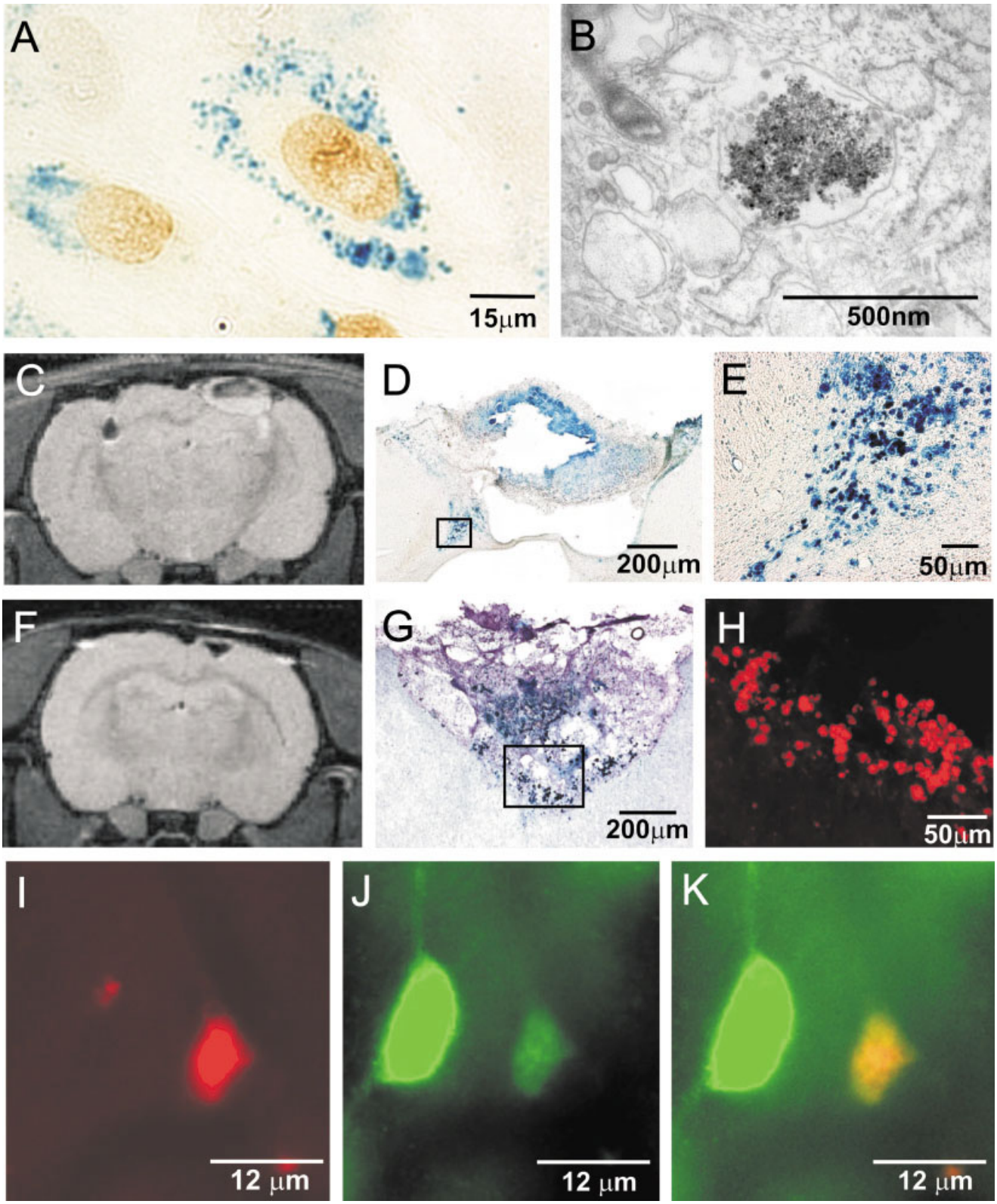

Fig. 4. Labeling of MSCs and their implantation into rats with a cortical photochemical lesion **A:** Cells in culture labeled with BrdU (brown), containing the contrast agent Endorem (Prussian blue staining). A cell labeled with iron oxide nanoparticles undergoing cell division, confirming that incorporation of nanoparticles does not adversely affect cell viability. **B:** Transmission electron microphotograph showing a cluster of iron oxide nanoparticles surrounded by a cell membrane, confirming the presence of iron inside the cell. **C:** T_2-weighted images of a cortical photochemical lesion and MSCs implanted into the contralateral hemisphere 2 weeks after implantation. The cell implant in the hemisphere contralateral to the lesion and the lesion itself are visible as hypointense areas. **D,E:** Histology performed 16 days postimplantation confirmed a large number of MSCs in the lesion (stained for Prussian blue). **F:** A hypointense signal in the lesion observed 30 days after intravenous injection of MSCs labeled with nanoparticles. **G:** Massive invasion of rat MSCs (Prussian blue staining, counterstained with hematoxylin) into a photochemical lesion 7 weeks after intravenous injection. **H:** Serial section stained for BrdU 7 weeks after intravenous injection. Implanted rat MSCs at the border of the lesion 4 weeks after grafting, doubly stained for BrdU (red; **I**) and the neuronal marker NeuN (green; **J**), coexpression of both markers appears as yellow (**K**).

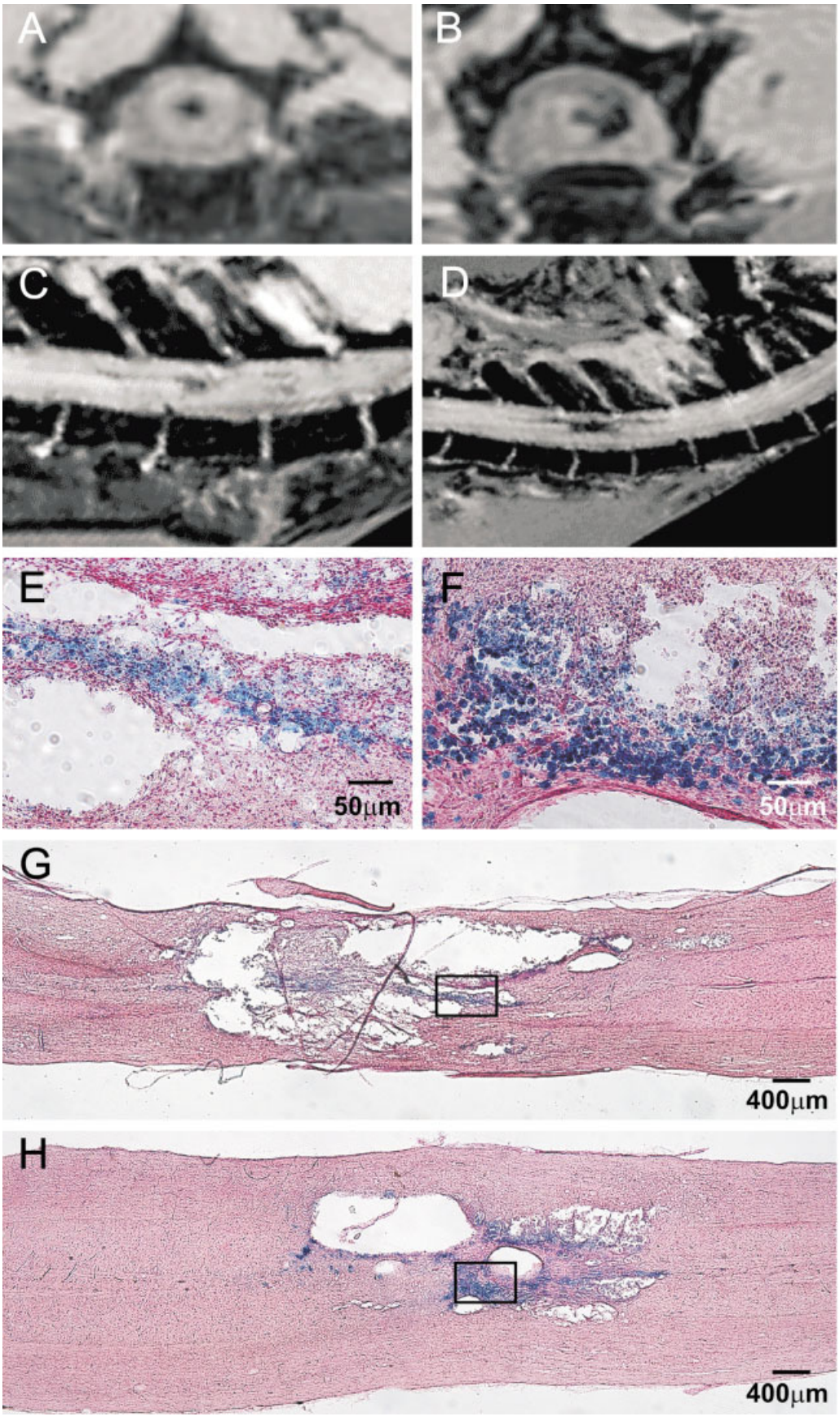

Fig. 5. MSCs labeled with nanoparticles implanted into rats with a spinal cord compression lesion. **A,C:** Tranversal and longitudinal sections of a spinal cord compression lesion on ex vivo MR images 5 weeks after compression. The lesion was detected as a hyperintensive area with a weak hypointense signal in the spinal cord channel within the lesion. **B,D:** Transversal and longitudinal images of a spinal cord compression lesion populated with intravenously implanted nanoparticle-labeled MSCs, 4 weeks after implantation. The lesion with nanoparticle-labeled cells is visible as a dark hypointensive area. **E,G:** Prussian blue staining of a spinal cord compression lesion. Only a few weakly stained Prussian blue-positive cells were found in the area of spinal cord lesion without cell implantation. **F,H:** Prussian blue staining of a spinal cord lesion with intravenously injected nanoparticle-labeled MSCs. The lesion was populated with Prussian blue-positive cells. Note the smaller lesion in implanted animals than in controls.

in lesioned spinal cord. In these experiments, the spinal cord was monitored ex vivo. Similarly, we were not able to obtain a clear MRI signal in vivo in animals with a spinal cord lesion because of noise derived from breathing.

Labeling cells with a contrast agent based on superparamagnetic nanoparticles before transplantation has been widely investigated for use in human medicine [intracellular iron labeling of human mononuclear cells (Sipe et al., 1999); labeling bone marrow haematopoietic progenitor cells (de Laquintane et al., 2002); labeling human mesenchymal stem cells and human cervical carcinoma cells by combining commercially available transfection agents with superparamagnetic iron oxide MRI contrast agents (Frank et al., 2003)]. Endorem is a contrast agent based on dextran-coated superparamagnetic iron oxide nanoparticles that is clinically approved as a blood pool agent. After further testing for cell toxicity and after verification of CNS tolerance, Endorem might meet criteria as a marker of implanted cells.

In our study we used ESCs and MSCs. Both types of cells have been successfully used in animal models of cell-based therapies. Mouse ES cell-derived glial precursors, transplanted into a rat with myelin disease, interact with the host neurons to produce myelin in the brain and spinal cord (Brustle et al., 1999). Retinoic acid-treated embryoid bodies from mouse ES cells, when transplanted into a rat spinal cord 9 days after traumatic injury, differentiated into astrocytes, oligodendrocytes, and neurons and promoted recovery (McDonald et al., 1999). Bjorklund et al. (2002) reported that undifferentiated mouse ES cells can become dopamine-producing neurons in the brain in a rat model of Parkinson's disease and can lead to partial functional recovery. An important issue in ES cell-based therapies might be the formation of tumors (McDonald et al., 1999). The ability of ESCs to form tumors in histocompatible animals reinforces the idea that it might be advantageous to use differentiated cells rather than stem cells for transplantation. To reduce the risk of tumor development after intracerebral injection, we induced neural differentiation in vitro by using ITSF medium. However, in 10% of experiments with intracerebral grafting, we observed tumor-like masses that originated from GFP-positive cells. We did not observe any formation of tumors in the lesion after intravenous injection, since the cell interactions leading to tumor formation may not be present. Because there was no difference in the number of cells populating the lesion between direct and intravenous applications, the latter might be a safer procedure for clinical use.

The use of MSCs in cell therapies may have some advantages over the use of other sources of cells: They are relatively easy to isolate (from bone marrow), they may be used in autologous transplantation protocols, and bone marrow as a source of cells has been already approved for the treatment of hematopoietic diseases. Various routes for the administration of MSCs have been tested. Kopen et al. (1999) injected MSCs into the lateral ventricle, and these cells migrated into the forebrain and cerebellum, including the striatum, the molecular layer of the hippocampus, the olfactory bulb, and the internal granular layer of the cerebellum. Li et al. (2001) and Lu et al. (2001) transplanted MSCs either directly into the striatum and cortex or intravenously into rats exposed to brain injury and focal cerebral ischemia. These cells migrated from the injection site and traveled to the boundary zone of the injury and the corpus callosum. In those studies, MSCs were expanded in vitro and administered either intraarterially or intravenously into rats with a traumatic brain injury. Cells migrated into the injury site, and the transplanted animals showed an improved neurological outcome in behavioral tests (Li et al., 2000; Lu et al., 2001; Hofstetter et al., 2002). The potential usefulness of MSCs may also include their secretion of different neuroactive molecules, insofar as nonhematopoietic bone marrow cells secrete interleukins, stem cell factor, and other hematopoietic regulatory molecules (Eaves et al., 1991; Maysinger et al., 1996), such as hematopoietic cytokine colony-stimulating factor-1, which is a growth factor in the CNS (Maysinger et al., 1996). It has been shown that human MSCs in culture respond to extracts from injured brain tissue by producing growth factors such BDNF, NGF, VEGF, and HGF (Chen et al., 2002). MSCs transplanted into the brain could therefore stimulate tissue regeneration, promote the recovery of function, and improve neurological deficits by mechanisms other than just direct neuronal replacement (Lu et al., 2001; Hofstetter et al., 2002; Chen et al., 2002).

Animal studies indicate that improved neural functioning can result from stem cell transplantation. With recent advances in human stem cell research, such as the successful propagation of ESC-derived (Thomson et al., 1998) and embryonic germ cell-derived human cells (Shamblott et al., 1998) and their derivation into a wide variety of cell lines, it may be possible in the future to achieve positive results in the treatment of human diseases. However, we have to take into account all necessary precautions before the full potential of cell therapy can be realized in patients suffering from degenerative diseases of the CNS or in patients with severe brain or spinal cord injuries. In particular, the lack of information about the behavior of transplanted ESCs in the host organism, about their influence outside the target structures, and about their potential neoplastic growth represent a serious obstacle to their therapeutic use. The labeling with iron oxide nanoparticles described here can help to elucidate the fate and effects of implanted stem cells, particularly in patients with brain or spinal cord injury.

CONCLUSIONS

We conclude that a commercially available contrast agent, Endorem, might be useful as a stem cell marker for the noninvasive in vivo MR tracking of cell fate following implantation. This study demonstrates that eGFP ESCs and MSCs labeled with iron oxide nanoparticles remain viable and migrate into an injured site; therefore, this procedure can be used to track implanted cells in experimental animals and presumably also in patients.

ACKNOWLEDGMENT

The authors are grateful to Guerbet (Roissy, France) for the generous gift of Endorem.

REFERENCES

Bjorklund A, Dunnett SB, Brundin P, Stoessl AJ, Freed CR, Breeze RE, Levivier M, Peschanski M, Studer L, Barker R. 2003. Neural transplantation for the treatment of Parkinson's disease. Lancet Neurol 2:437–445.

Bjorklund LM, Sanchez-Pernaute R, Chung S, Andersson T, Chen IY, McNaught KS, Brownell AL, Jenkins BG, Wahlestedt C, Kim KS, Isacson O. 2002. Embryonic stem cells develop into functional dopaminergic neurons after transplantation in a Parkinson rat model. Proc Natl Acad Sci USA 99:2344–2349.

Brustle O, Jones KN, Learish RD, Karram K, Choudhary K, Wiestler OD, Duncan ID, McKay RD. 1999. Embryonic stem cell-derived glial precursors: a source of myelinating transplants. Science 285:754–756.

Bulte JW, Bryant LHJ. 2001. Molecular and cellular magnetic resonance contrast agents. In: De Cuyper M, Bulte JW, editors. Physics and chemistry basis of biotechnology. Dordrecht, The Netherlands: Kluwer Academic Publishers. p 197–211.

Bulte JW, Brooks RA, Moskowitz BM, Bryant LHJ, Frank JA. 1999a. Relaxometry and magnetometry of the MR contrast agent MION-46L. Magn Reson Med 42:379–384.

Bulte JW, Zhang SC, van Gelderen P, Herynek V, Jordan EK, Duncan ID, Frank JA. 1999b. Neurotransplantation of magnetically labeled oligodendrocyte progenitors: magnetic resonance tracking of cell migration and myelination. Proc Natl Acad Sci USA 96:15256–15261.

Bulte JW, Douglas T, Witwer B, Zhang SC, Strable E, Lewis BK, Zywicke H, Miller B, van Gelderen P, Moskowitz BM, Duncan ID, Frank JA. 2001. Magnetodendrimers allow endosomal magnetic labeling and in vivo tracking of stem cells. Nat Biotechnol 19:1141–1147.

Chen X, Katakowski M, Li Y, Lu D, Wang L, Zhang L, Chen J, Xu Y, Gautam S, Mahmood A, Chopp M. 2002. Human bone marrow stromal cells cultures conditioned by traumatic brain tissue extracts: growth factor production. J Neurosci Res 69:687–691.

de Laquintane BD, Dousset V, Solanilla A, Petry KG, Ripoche J. 2002. Iron particle labeling of haematopoietic progenitor cells: an in vitro study. Biosci Rep 22:549–554.

Doetschman TC, Eistetter H, Katz M, Schmidt W, Kelmer R. 1985. The in vitro development of blastocyst-derived embryonic stem cell lines: formation of visceral yolk sac, blood islands and myocardium. J Embryol Exp Morphol 87:27–45.

Eaves CJ, Cashman JD, Kay RJ, Dougherty GJ, Otsuka T, Gaboury LA, Hogge DE, Lansdorp PM, Eaves AC, Humphries RK. 1991. Mechanisms that regulate the cell cycle status of very primitive hematopoietic cells in long-term human marrow cultures. II. Analysis of positive and negative regulators produced by stromal cells within the adherent layer. Blood 78:110–117.

Frank JA, Miller BR, Arbab AS, Zywicke HA, Jordan EK, Lewis BK, Bryant LH, Jr., Bulte JW. 2003. Clinically applicable labeling of mammalian and stem cells by combining superparamagnetic iron oxides and transfection agents. Radiology 228:480–487.

Franklin RJ, Blaschuk KL, Bearchell MC, Prestoz LL, Setzu A, Brindle KM, ffrench-Constant C. 1999. Magnetic resonance imaging of transplanted oligodendrocyte precursors in the rat brain. Neuroreport 10:3961–3965.

Gage FH. 2002. Neurogenesis in the adult brain. J Neurosci 22:612–613.

Hawrylak N, Ghosh P, Broadus J, Schlueter C, Greenough WT, Lauterbur PC. 1993. Nuclear magnetic resonance (NMR) imaging of iron oxide-labeled neural transplants. Exp Neurol 121:81–92.

Hoehn M, Kustermann E, Blunk J, Wiedermann D, Trapp T, Focking M, Arnold H, Hescheler J, Fleischmann BK, Buhrle C. 2002. Monitoring of implanted stem cell migration in vivo: a highly resolved in vivo magnetic resonance imaging investigation of experimantal stroke in rat. Proc Natl Acad Sci USA 100:1073–1078.

Hofstetter CP, Schwarz EJ, Hess D, Widenfalk J, El Manira A, Prockop JD, Olson L. 2002. Marrow stromal cellsform guiding strands in the injured spinal cord and promote recovery. Proc Natl Acad Sci USA 96:2199–2204.

Isacson O. 2003. The production and use of cells as therapeutic agents in neurodegenerative diseases. Lancet Neurol 2:417–424.

Jendelová P, Herynek V, De Croos J, Glogarová K, Andersson B, Hájek M, Syková E. 2003. Imaging the fate of implanted bone marrow stromal cells labeled with superparamagnetic nanoparticles. Magn Reson Med 50:767–776.

Kopen GC, Prockop DJ, Phinney DG. 1999. Marrow stromal cells migrate throughout forebrain and cerebellum, and they differentiate into astrocytes after injection into neonatal mouse brains. Proc Natl Acad Sci USA 96:10711–10716.

Li Y, Chopp M, Chen J, Wang L, Gautam SC, Xu YX, Zhang Z. 2000. Intrastriatal transplantation of bone marrow nonhematopoietic cells improves functional recovery after stroke in adult mice. J Cereb Blood Flow Metab 20:1311–1319.

Li Y, Chen J, Chen J, Wang L, Lu M, Chopp M. 2001. Treatment of stroke in rat with itracarotid administration of marrow stromal cells. Neurology 56:1666–1672.

Lu D, Mahmood A, Wang L, Li Y, Lu M, Chopp M. 2001. Adult bone marrow stromal cells administered intravenously to rats after traumatic brain injury migrate into brain and improve neurological outcome. Neuroreport 12:559–563.

Maysinger D, Berezovskaya O, Fedoroff S. 1996. The hematopoietic cytokine colony stimulating factor 1 is also a growth factor in the CNS: (II). Microencapsulated CSF-1 and LM-10 cells as delivery systems. Exp Neurol 141:47–56.

McDonald JW, Liu XZ, Qu Y, Liu S, Mickey SK, Turetsky D, Gottlieb DI, Choi DW. 1999. Transplanted embryonic stem cells survive, differentiate and promote recovery in injured rat spinal cord. Nat Med 5:1410–1412.

Norman AB, Thomas SR, Pratt RG, Lu SY, Norgren RB. 1992. Magnetic resonance imaging of neural transplants in rat brain using a superparamagnetic contrast agent. Brain Res 594:279–283.

Pachernik J, Esner M, Bryja V, Dvorak P, Hampl A. 2002. Neural differentiation of mouse embryonic stem cells grown in monolayer. Reprod Nutr Dev 42:317–326.

Paxinos G, Watson C. 1986. The rat brain in stereotaxic coordinates. Sydney: Academic Press.

Shamblott MJ, Axelman J, Wang S, Bugg EM, Littlefield JW, Donovan PJ, Blumenthal PD, Huggins GR, Gearhart JD. 1998. Derivation of pluripotent stem cells from cultured human primordial germ cells. Proc Natl Acad Sci USA 95:13726–13731.

Silani V, Leigh N. 2003. Stem therapy for ALS: hope and reality. Amyotroph Lateral Scler Other Motor Neuron Disord 4:8–10.

Sipe JC, Filippi M, Martino G, Furlan R, Rocca MA, Rovaris M, Bergami A, Zyroff J, Scotti G, Comi G. 1999. Method for intracellular magnetic labeling of human mononuclear cells using approved iron contrast agents. Magn Reson Imaging 17:1521–1523.

Taupin P, Gage FH. 2002. Adult neurogenesis and neural stem cells of the central nervous system in mammals. J Neurosci Res 69:745–749.

Thomson JA, Itskovitz-Eldor J, Shapiro SS, Waknitz MA, Swiergiel JJ, Marshall VS, Jones JM. 1998. Embryonic stem cell lines derived from human blastocysts. Science 282:1145–1147.

van Praag H, Schinder AF, Christie BR, Toni N, Palmer TD, Gage FH. 2002. Functional neurogenesis in the adult hippocampus. Nature 415:1030–1034.

Vanicky I, Urdzikova L, Saganova K, Cizkova D, Galik J. 2001. A simple and reproducible model of spinal cord injury induced by epidural balloon inflation in the rat. J Neurotrauma 18:1399–1407.

Wang YX, Hussain SM, Krestin GP. 2001. Superparamagnetic iron oxide contrast agents: physicochemical characteristics and applications in MR imaging. Eur Radiol 11:2319–2331.

Watson BD, Dietrich WD, Busto R, Wachtel MS, Ginsberg MD. 1985. Induction of reproducible brain infarction by photochemically initiated thrombosis. Ann Neurol 17:497–504.

Weissleder R, Cheng HC, Bogdanova A, Bogdanov A Jr. 1997. Magnetically labeled cells can be detected by MR imaging. J Magn Reson Imaging 7:258–263.

Yeh T, Zhang W, Ildstad ST, Ho C. 1993. Intracellular labeling of T-cells with superparamagnetic contrast agents. Magn Reson Med 30:617–625.

Yeh T, Zhang W, Ildstad ST, Ho C. 1995. In vivo dynamic MRI tracking of rat T-cells labeled with superparamagnetic iron oxide particles. Magn Reson Med 33:200–208.